

Line of multicritical Lifshitz points in the phase diagram of MnP

C. C. Becerra, H. J. Brumatto, and N. F. Oliveira, Jr.

Instituto de Física, Universidade de São Paulo, Caixa Postal 66318 - CEP 05389-970 São Paulo, Brazil

(Received 3 June 1996)

Lifshitz critical behavior has been reported in the orthorhombic magnetic system MnP which exhibits uniaxial Ising-type Lifshitz points (LP's). Two LP's have been previously identified in the phase diagram of MnP. One when the external magnetic field \mathbf{H} was applied along the intermediate anisotropy axis \mathbf{b} , the other when \mathbf{H} was along the hard axis \mathbf{a} . Both LP's occurs roughly at the same temperature ($T_L \sim 120$ K) but at different values of \mathbf{H} because of the difference in anisotropy along these axes. In this work we report on measurements made with \mathbf{H} applied within the \mathbf{ab} plane, at 20° and 45° from the b axis. The observed phase diagram shows, near the confluence of the modulated and ferromagnetic phases with the paramagnetic phase, the same characteristics of the phase boundaries found for $\mathbf{H} \parallel \mathbf{a}$ and $\mathbf{H} \parallel \mathbf{b}$. An analysis of the crossover exponent ϕ , obtained from the shape of the phase boundaries near the confluence point gave $\phi = 0.61 \pm 0.02$, and $T_L = 119.9$ K. These values are consistent with those found when \mathbf{H} is along the \mathbf{a} and the \mathbf{b} axes. This result indicates that there is a line of Lifshitz multicritical points connecting the two previously found LP's. [S0163-1829(96)03045-7]

I. INTRODUCTION

Manganese phosphide (MnP) is a unique material. Its magnetic phase diagram exhibits several ordered phases, including different kinds of modulated phases. It is the only magnetic system in which a pure Lifshitz-type critical behavior¹ has been found and critical exponents measured.²⁻⁴ Crossover from Lifshitz to Ising critical behavior and other types of critical points have also been found. Besides this, evidence of the existence of a region of commensurate-incommensurate transitions in the phase diagram was given⁵ and the influence of nonmagnetic impurities in the magnetic phase transitions studied.⁶ The richness of its magnetic behavior, the phase transitions and the observed critical points can be simply explained in terms of the competition between ferromagnetic and antiferromagnetic interactions in the system.^{8,9} Thus, MnP is not only the prototype of a magnetic system in which Lifshitz critical behavior can be experimentally explored but is also an excellent system to study magnetic behavior related to modulated magnetic phases.

The Lifshitz multicritical point (LP) occurs in a magnetic system at the confluence of a ferromagnetic (F) and a modulated ordered phase with the paramagnetic (P) phase. Transition from the ordered phases to the P phase are second order. The LP divides this second-order (λ) line in two segments. Along the modulated segment of this λ , line the wave vector \mathbf{q} associated with the magnetic order goes continuously to zero as the LP is approached.

Phase diagram and multicritical points in MnP

MnP has an orthorhombic structure ($a = 5.92$; $b = 5.26$; $c = 3.17$ Å) and becomes ferromagnetic at 291 K, with its magnetic moments aligned along the c (easy) axis. When cooled below 47 K a first-order transition to a spiral (screw) phase takes place. In this modulated phase, the Mn magnetic moments are confined within the \mathbf{bc} planes that are perpendicular to the \mathbf{a} axis. The magnetic moments are parallel

inside these \mathbf{bc} planes but moving along the \mathbf{a} axis a rotation of the magnetization direction inside the \mathbf{bc} plane occurs from plane to plane. That is the wave vector \mathbf{q} points along the \mathbf{a} axis. At $T = 4$ K a full rotation is completed roughly each $9a$.² In Fig. 1 we sketch the phase diagram of MnP obtained when the magnetic field \mathbf{H} is applied along the intermediate anisotropy \mathbf{b} axis and also along the hard \mathbf{a} axis.

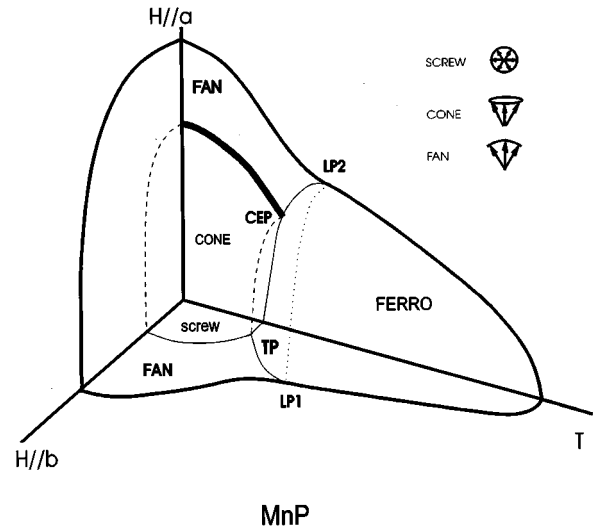


FIG. 1. Sketch of the magnetic phase diagram of MnP in the $H \parallel a$, $H \parallel b$ vs T space. The dotted line at $T \sim 120$ K links the Lifshitz points (LP's) that occur when H lies along the \mathbf{a} and \mathbf{b} directions. The dashed line ~ 45 K connects the critical end point (CEP) observed when $H \parallel a$ with the triple point (TP) in the phase diagram with $H \parallel b$. Transitions between the ordered phase and the paramagnetic phase are second order. Transitions between the ordered phases are first order except for the CONE-FAN boundaries for $H \parallel a$ that is second order and ends at a CEP. Sketches of the magnetic moment configuration of the modulated phases are given. They should be viewed as the projection of the moments in successive \mathbf{bc} planes into a single point.

This outline is based on the data of Refs. 2 and 7. For \mathbf{H} applied along the \mathbf{b} axis it is seen that in addition to the ferro (F) and screw (SCR) phases another modulated phase called ‘‘FAN’’ is present for higher values of H . In this phase the wave vector \mathbf{q} is also parallel to the \mathbf{a} axis. The difference with the SCR phase is that here the magnetic moments do not perform a full rotation in the \mathbf{bc} planes as we move along the \mathbf{a} direction but instead they oscillate about the \mathbf{b} axis like a *fan*. This fan closes with increasing field until an upper critical field is reached. All transitions between the ordered phases are first order and the transitions to the paramagnetic (P) phase are of second order. Figure 1 also shows the outline of the phase diagram obtained when \mathbf{H} is applied along the hard anisotropy axis \mathbf{a} . Both phase diagrams have similarities, but the phase boundaries in this last case occur at higher fields because of the stronger anisotropy involved in this direction. Here also two modulated phases occur. Due to the absence of neutron-diffraction information for this field configuration these phases were tentatively identified as a ‘‘CONE’’ and a ‘‘FAN’’ phase.⁷ In this latter case however the boundary between the two modulated phase (CONE-FAN) was found to be a line of second-order transitions terminating at a critical end point (CEP).¹⁰ The strongest similarity with the $H\parallel b$ case occurs at the confluence of the ferromagnetic and the FAN phases with the paramagnetic phase. In both cases this point occurs roughly at the same temperature (121 ± 1 K) and there, the phases boundaries meet with the same tangent. For $H\parallel b$ this point was the first experimental observation of a Lifshitz multicritical point (LP).^{1,2} In fact, both points have been shown to be LP’s. These LP’s are of the uniaxial type ($d=3$, $n=1$, $m=1$), where d , n , and m are, respectively, the spatial, spin, and wave vector dimensionalities. The shape of the phase boundaries near a multicritical is governed by the crossover exponent ϕ through the form $p\sim|t|^\phi$ where p and t are scaling fields that are linear combinations of T and H .^{1,2} Theoretical predictions give $\phi=0.625$.¹¹ The experimental analysis of the phase boundaries for MnP close to the multicritical point gave $\phi=0.63\pm 0.04$ at the LP for $H\parallel b$,² and 0.64 ± 0.02 for the LP occurring for $H\parallel a$.⁷ Other LP critical exponents have been obtained for $H\parallel b$. These are the exponent β related to the vanishing of the wave vector \mathbf{q} as the LP is approached, and the exponent α related to the specific heat. From neutron data it was found $\beta=0.480\pm 0.013$,³ which is near the theoretically predicted (0.50) to first order in the ϵ expansion.¹² Experimentally it was found that $\alpha=0.46\pm 0.03$.⁴ The expected value for the LP in MnP is in the range 0.42 to 0.49.⁴

The existence of these two Lifshitz points raises the question of their connection. In this paper we investigate the phase boundaries in the temperature region around the LP’s when the external field is directed along intermediates directions contained in the \mathbf{ab} plane. We found that our data is consistent with the existence of a line of Lifshitz multicritical points connecting the two previously observed when H was applied along the \mathbf{b} and \mathbf{a} axis. This is an experimental observation of a line of multicritical Lifshitz points. This paper is arranged as follows: In Sec. II we give the relevant experimental information; in Sec. III the experimental results are shown, and in Sec. IV we present the analysis and discussion of the results.

II. EXPERIMENTS AND SAMPLE

A spherical single crystal of MnP with 5.2 mm of diameter was used in all the ac magnetic-susceptibility measurements. This ensured a homogeneous internal field and as a consequence sharp phase transitions were obtained. The sample was mounted at the end of a rod that was inserted inside the pickup coils. The temperature was measured with a calibrated carbon-glass resistor mounted on the rod. The thermometer was in direct contact with the sample. Fields \mathbf{H} up to 70 kOe were obtained with a superconducting magnet. The experimental setup is described in Ref. 2. In this setup the temperature could be varied from 1.2 K to room temperature and maintained constant within 0.01 K for long periods of time. The superconducting magnet can be tipped around its vertical axis. The maximum permitted tipping angle is 4° . We will see that this last feature is very important for our experiments since it will permit a good alignment of the desired direction in the crystal with the external applied field. The tipping mechanism is described in Ref. 7.

The ac susceptibility (χ) measurements were performed using the experimental setup described in Ref. 2. The amplitude and frequency of the modulation field \mathbf{h} were 10 Oe and 155 Hz, respectively. The field was applied along the direction of the external field \mathbf{H} of the superconducting magnet.

All the runs were made at fixed temperature, the field was varied at a slow rate (typically 7 Oe/s). The orientation of the sample in the magnetic field was done in two steps. First the desired direction in the sample was aligned with the aid of x ray. The sample was then glued with GE varnish to the measuring rod. We estimate to within 1° the alignment between the selected direction and field in this first step. In the second step the sample was oriented inside the experimental setup. In this procedure we use the shape of the experimental curves as a guide to obtain the final orientation. The goal was to eliminate any component of the field along the \mathbf{c} axis of the sample. Since the \mathbf{c} axis is the easy axis in the ferromagnetic phase, a magnetic field applied along this direction acts as an ordering field and destroys the transition from the ferromagnetic phase to the paramagnetic one. This point was discussed in Ref. 2. A true second-order transition is only observed when the field is totally contained in the plane perpendicular to the easy axis. In the susceptibility curves this transition is seen as a sharp λ -like singularity. A small component of the field along the \mathbf{c} axis will cause a rounding of the curve and a shift of the ‘‘pseudo’’ transition to lower fields. This final adjustment was done at a temperature just above that corresponding to the LP to ensure that we had a ferro-para transition. The susceptibility versus field curve was monitored while the magnet was progressively tipped. The tipping in which the sharpest transition along the ferro-paramagnetic boundary was observed was selected. This sharpest λ like peak also corresponds to the highest transition field.

Experiments in which the field was applied at 20° and 45° from the \mathbf{b} axis in the \mathbf{ab} plane were performed. The most extensive set of experimental data was taken at 45° .

III. EXPERIMENTAL RESULTS

Figures 2 and 3 show some of the data obtained when the external applied field is in the \mathbf{ab} plane at an angle $\theta=45^\circ$

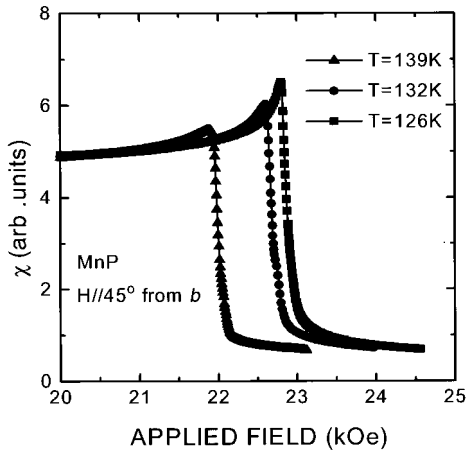


FIG. 2. Susceptibility χ vs H curves for three temperatures above 120 K. The field H was applied at 45° from the \mathbf{a} and \mathbf{b} axes in the \mathbf{ab} plane of the crystal. Note the sharpening of the λ -like singularity when the temperature is lowered.

with the axis. Different temperature ranges are covered in each of these figures. The observed transitions correspond to distinct phase boundaries. The data (not shown) obtained for $\theta=20^\circ$ are qualitatively similar.

Figure 2 shows representative susceptibility curves near the F-P transition. The temperatures are above that corresponding to the observed LP when the field is applied either along the \mathbf{b} or \mathbf{a} axes. The λ -like shape of the curves is indicative of a second-order transition to the paramagnetic phase, the anomaly is sharper close to the LP temperature. This is due, as explained in Ref. 4, to the crossover from the Ising to the Lifshitz critical behavior of the specific-heat exponent as the LP is approached.

Figure 3 contains examples of the data obtained near the confluence of the F, FAN, and P phases and also well below

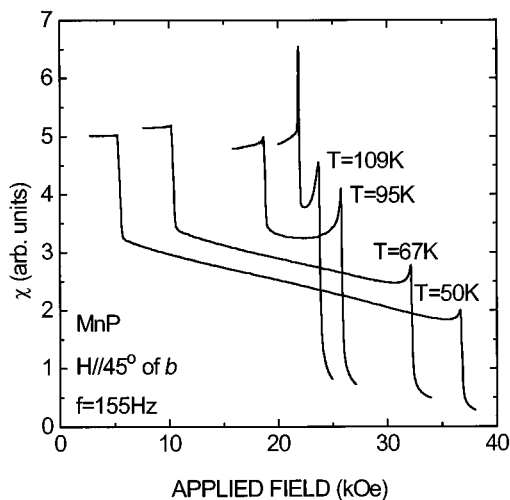


FIG. 3. Susceptibility χ vs H obtained for several temperatures below 120 K. The field was applied at 45° from the \mathbf{a} and \mathbf{b} axes in the \mathbf{ab} plane of the crystal. Transitions at lower fields are first order. The λ -like transition at the higher fields corresponds to the second-order transition between the FAN and paramagnetic phases.

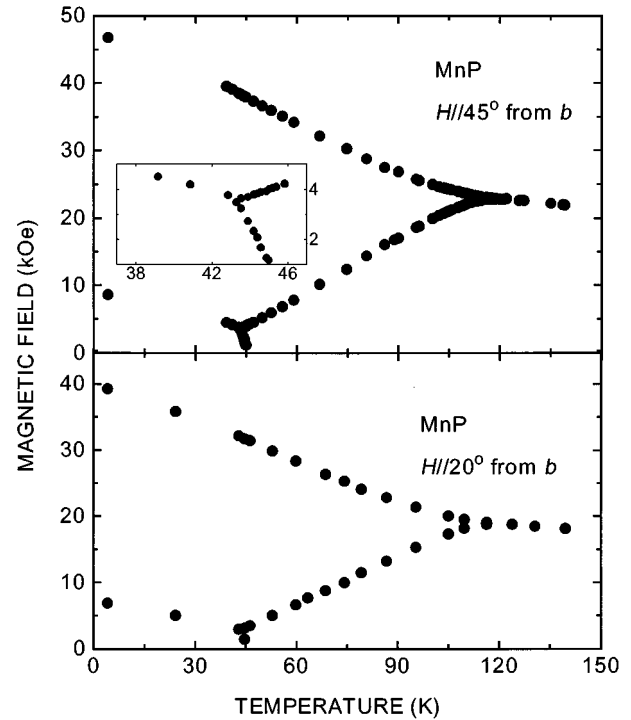


FIG. 4. Overall view of the phase diagrams measured when the field was applied at 45° and 20° of the \mathbf{b} axis in the \mathbf{ab} plane. The inset shows the region close to the triple point where the screw (SCR), fan (FAN), and ferromagnetic (FERRO) phases meet.

the LP temperature. There other phase transitions occurs. The transitions from the FAN to the P are clearly marked by a λ peak in χ . The sharp peak at the lower field, followed by a significant decrease in χ , corresponds to the first-order transition between the F and FAN phases. At lower temperatures the distinctive peak of the F-FAN transition disappears and the sudden drop in χ remains as the sign of the phase transition. This occurs as explained in Ref. 5, because the hysteresis at this first-order transition increases with decreasing temperature and the amplitude of the ac modulation field (of a few Oe) becomes smaller than the hysteresis width.

The F-FAN transition field H_1 was taken at the maximum of the sharp susceptibility spike or, in the curves obtained at the lower temperatures, at the point where the sudden decrease in dM/dH begin. For the FAN-P transition field H_λ and the F-P transition field H'_λ two choices for the fields can be made. Either at the maximum of the λ -like peak or at the intersection of the two tangents to the curves drawn just below and above the transition. These two fields differ roughly by 0.1% and the choice did not have any detectable influence on the outcome of the analysis. Since some small rounding is always present at the λ transition (see Figs. 2 and 3), we choose the two tangents method to determine the corresponding field.

Figure 4 shows the phase boundaries obtained using the criteria described above, for the two directions measured in the \mathbf{ab} plane. In the inset of Fig. 4 the region near the meeting of the three ordered phases, around 45 K, is detailed for the case in which $\theta=45^\circ$. No correction for demagnetization field was applied. Estimates indicate that the internal fields are roughly 1% lower than the applied field shows in the

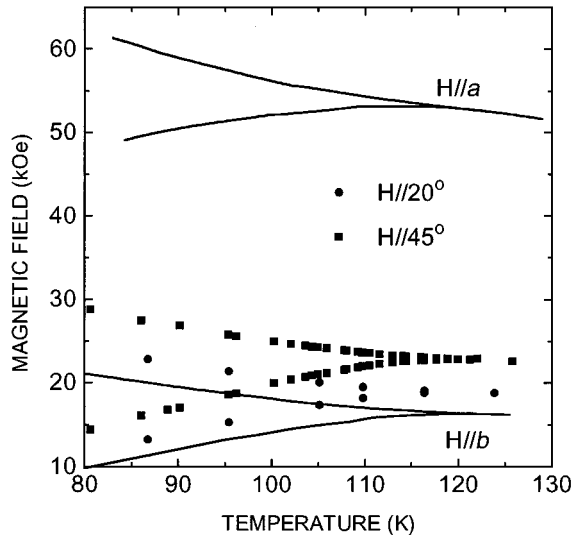


FIG. 5. Data obtained for H applied at 45° and 20° from the b axis and close to the region in temperature around 120 K. For comparison, we also depict the previously reported phase boundaries near the LP's when H was applied along the b and a crystal axes.

figure. This correction will not affect significantly the result of the analysis. The data near the LP obtained for the 20° and 45° configuration are plotted in detail in Fig. 5. In the same figure data for the configuration in which the field is applied along the b and also along the a axes obtained from Refs. 2 and 7 are included for comparison.

IV. DISCUSSION

In MnP the existence of the modulated phases has been interpreted in terms of the competition of ferromagnetic (J_1) and antiferromagnetic (J_2) phenomenological exchange interactions that occur along the a axis,^{8,9} the ratio $\kappa = J_1/J_2$ is found to be a function of the temperature. These data were obtained from the analysis of neutron-diffraction measurements of spin-wave dispersion curves. In this analysis, it was assumed that the Mn ions are coupled ferromagnetically inside a bc plane, that the coupling with ions in nearest-neighbors planes perpendicular to the a axis is also ferromagnetic with $J_1 > 0$ and with Mn atoms in next-neighbors planes is antiferromagnetic with $J_2 < 0$. The resulting analysis shows that the ratio κ varies from $\kappa = -0.23$ at 200 K to $\kappa = -0.27$ at 70 K. This ratio is also virtually not changed by an applied magnetic field \mathbf{H} .⁸ It is well known that such competing interactions give rise to modulated structures when their ratio exceeds $\kappa = -0.25$ (a mean-field result). In MnP this value of ratio occurs around 120 K, the temperature where the LP is observed. This is what makes MnP a unique system, since it is naturally tuned around this critical value of κ . Since κ is T dependent the temperature plays the role of the κ variable in the corresponding theoretical phase diagrams of systems with competing exchange that exhibits a LP. The role of the thermal axis is played by the magnetic field as discussed in Ref. 2. A simple model that is relevant to MnP and that exhibits a LP at the ratio $\kappa = -0.25$ is the anisotropic next-nearest-neighbors Ising model.¹³ The LP of

this model is of the same universality class as that found in MnP.¹⁴

Figures 4 and 5 show that the phase diagrams obtained for both intermediate directions between the a and b axes are qualitatively similar to the phase diagram obtained when \mathbf{H} is applied along the b axis. It is clear that a triple point (TP) in which phase boundaries meet with distinct slopes is present. In the inset of Fig. 4 a blowup of this region is shown for \mathbf{H} forming 45° with the a and b axes. Note that all angles are less than 180° . This suggests that the transition to the behavior found when $H \parallel a$ with a second-order line separating the two modulated phases and ending at a CEP, should occur closer to the a direction. A line of triple points starting at $H \parallel b$ should be converted into a line of CEP, ending at $H \parallel a$ (dashed line in Fig. 1). A tricritical point may occur in this case. The other characteristics of the phase diagrams are very similar to those observed along the a and b directions. An increase in the transition fields along all the phase boundaries is observed. This can be accounted for by the increase in anisotropy present when we move from the b towards the a direction.

In the obtained phase diagrams the confluence of the modulated fan phase with the ferromagnetic and the paramagnetic phases occurs around 120 K, the temperature associated with the two previously identified LP's. See Fig. 5 for a comparative plot of our results with those previously reported for the LP.

The analysis of the critical behavior of the phase boundaries near the Lifshitz point is usually done by introducing the appropriate scaling axes.² Near the multicritical point the boundaries obey the relation $t = C|p|^{1/\phi}$ where p and t are the scaling axes and ϕ the crossover exponent. The usual procedure is to choose the p axis tangent to the phase boundary at the multicritical point (MP).¹⁵ The t scaling axis can be taken along any other direction but the optimal choice is to select one for which the range of the fit to the above relation is maximized: Here we choose, as outlined in Refs. 1 and 2, the t axis as parallel to the field axis. The origin of the scaling axes is selected at the MP. We refer to Fig. 17 of Ref. 2 for a sketch of the scaling axes in this case.

As discussed in Refs. 1, 2 we assume that all the phase boundaries, including the first-order one obey the same equation with different amplitudes C but with the same crossover exponent ϕ . We adopt here the simplifying assumption that the p axis is parallel to the temperature axis $p = (T - T_L)/T_L$, (see Figs. 4 and 5 to verify that this assumption is well satisfied). This procedure was already applied in Refs. 1, 2, and 7. As commented above, the t axis is taken as parallel to the magnetic field $t = (H - H_L)/H_L$. It follows from these assumptions that at a given T below the LP temperature the difference between the values of the second-order transition field H_λ between the FAN-P phases and the first-order ferro-FAN transition field H_1 follows the relation $H_\lambda - H_1 = B(T_L - T)^{1/\phi}$.

The analysis of the behavior of the phase boundaries below but near the LP was done through a least-squares fit to $H_\lambda - H_1 = B(T_L - T)^{1/\phi}$. The analysis was mostly done on the data for the configuration where the field was applied at 45° to the a and b axes because this set of data is more extensive. We did fits with different numbers of experimental points that were in a range of temperatures extending from a mini-

TABLE I. Results for the different fits applied to the data for H at 45° from the **a** and **b** axes. The columns correspond to the temperature range specified by T_{\min} , the number of points included in the fit, the best T_L , and the best crossover exponent ϕ .

Fit no.	Range T_{\min}	Data points	T_L (K)	Φ
1	90.1	22	119.5	0.6352
2	95.3	21	119.6	0.6265
3	96.2	20	119.7	0.6196
4	100.2	19	119.8	0.6129
5	102.1	18	120.2	0.5809
6	103.6	17	120.4	0.5633

imum temperature T_{\min} to the temperature that includes the point closest to the LP. For each range several fits were done in which T_L was fixed and B and ϕ were the fitted parameter. The value of T_L was changed in one-tenth of a degree increments and for each range; the T_L for which the analysis gave the best fit was selected. Table I summarizes the results of the fits for the six ranges selected. The minimum temperature T_{\min} , the number of points included the best value of T_L found for each range as well as the crossover exponent obtained for this best T_L are shown. Taking a weighted mean of these results using the dispersions of the fits as weighting factor we obtain for this 45° configuration $T_L=119.9\pm 0.4$, and $\phi=0.61\pm 0.02$. A similar analysis applied to the less extensive set of data obtained for H at 20° from the **b** axis in the **ab** plane gave: $\phi=0.60\pm 0.02$ when T_L was fixed at 119.9 K. The results of these fits are graphically plotted in Fig. 6 where the width of the FAN phase $H_\lambda - H_1$ is plotted against T . The solid lines were traced with the best-fit values. The obtained values for T_L and ϕ are consistent with those measured for the field applied along the intermediate **b** and hard **a** anisotropy axes. This strongly suggests that the Lifshitz point behavior observed when the external field is applied along these two principal directions is shared also by the intermediate directions contained in the **ab** plane and that we are in the presence of a line of multicritical Lifshitz points.

V. CONCLUSIONS

We measured the magnetic phase diagram of MnP when the external magnetic field was applied along two directions contained in the crystallographic **ab** plane and forming, respectively, angles of 20° and 45° with the b axis. The obtained phase diagram is very similar to the measured one when the field is applied along the intermediate anisotropy

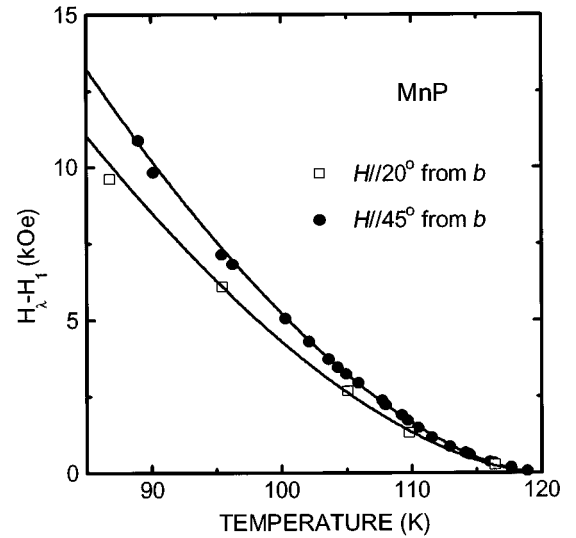


FIG. 6. The solid curve represents the best fit obtained for the phase boundaries near the multicritical point for the two directions of the applied field. The width of the FAN phase at a given T is the fitted quantity (see text). The values of the parameters are quoted in the text.

axis **b**. In particular in the region of the confluence of the modulated, ferromagnetic, and paramagnetic phases the analytic behavior found for the phase boundaries measured through the crossover exponent ϕ is the same as that obtained when the field is applied along the **b** and also along the **a** axis. This is strong experimental evidence that the two Lifshitz points previously found when **H** was applied along these two principal directions are connected by a line of multicritical Lifshitz points.

The triple point that occurs when the three ordered phases meet when $H\parallel b$ is also observed when the field makes a 45° with this axis. This implies that the possible occurrence of a tricritical point (i.e., at the connection of the line of first-order points with the segment of the line of critical end points) should occur closer to the **a** direction. This is presently under investigation.

ACKNOWLEDGMENTS

We express our thanks for the financial support of the following Brazilian Agencies: Conselho Nacional de Pesquisas (CNPq) under Grants No. 304067/77-9 and 500626/92-8; Fundação de Amparo à Pesquisa do Estado de São Paulo, Grant No. 92/0845-2; Financiadora de Estudos e Projetos (FINEP).

¹C. C. Becerra, Y. Shapira, N. F. Oliveira, Jr., and T. S. Chang, Phys. Rev. Lett. **44**, 1692 (1980).

²Y. Shapira, C. C. Becerra, N. F. Oliveira, Jr., and T. S. Chang, Phys. Rev. B **24**, 2780, (1981).

³R. H. Moon, J. M. Cable, and Y. Shapira, J. Appl. Phys. **52**, 2025 (1981).

⁴V. Bindilatti, C. C. Becerra, and N. F. Oliveira, Jr., Phys. Rev. B **40**, 9412 (1989).

⁵C. C. Becerra, N. F. Oliveira, Jr., and Y. Shapira, J. Phys. (Paris) Colloq. **49**, C8-895 (1988).

⁶C. C. Becerra, A. Zieba, N. F. Oliveira, Jr., and H. Fjellvag, J. Appl. Phys. **67**, 5442 (1990).

- ⁷Y. Shapira, N. F. Oliveira, Jr., C. C. Becerra, and S. Foner, Phys. Rev. B **29**, 361 (1984).
- ⁸K. Tajima, Y. Ishikawa, and H. Obara, J. Magn. Mater. **15-18**, 373 (1980).
- ⁹H. Yoshikawa, S. M. Shapiro, and T. J. Komatsubara, J. Phys. Soc. Jpn. **54**, 3084 (1985).
- ¹⁰C. C. Becerra, A. C. Migliano, and N. F. Oliveira, Jr., J. Appl. Phys. **63**, 3092 (1988).
- ¹¹D. Mukamel and M. Luban, Phys. Rev. B **18**, 3631 (1978)
- ¹²R. M. Hornreich, M. Luban, and S. Shtrickman, Phys. Rev. Lett. **35**, 1678 (1975).
- ¹³W. Selke, Phys. Rep. **180**, 213 (1988).
- ¹⁴C. Yokoi, M. D. Coutinho Filho, and S. R. Salinas, Phys. Rev. B **24**, 4047 (1981); **24**, 5430 (1981); **29**, 6341 (1984).
- ¹⁵R. B. Griffiths and J. C. Wheeler, Phys. Rev. A **2**, 1047 (1970).